Journal of Inflammation Research

Dovepress
open access to scientific and medical research

Open Access Full Text Article

ORIGINAL RESEARCH

She-Chuang-Si-Wu-Tang Alleviates Inflammation and Itching Symptoms in a Psoriasis Mouse Model by Regulating the Th17/IL-17 Axis via the STAT3/MAPK Pathways

Weixiong Chen[1,2,*], Jianqiang Liang[3,*], Shuang He[1,4,5], Qingsong Liang[1,4,5], Wenting Tian[6], Aobo Lu[1], Demin Li[1], Zhicheng Huang[1], Guanyi Wu[1,4,5]

[1]College of Basic Medicine, Guangxi University of Chinese Medicine, Nanning, Guangxi, 530299, People's Republic of China; [2]School of Health Science and Engineering, University of Shanghai for Science and Technology, Shanghai, 200093, People's Republic of China; [3]Department of Dermatology, the First People's Hospital of Yulin, Yulin, Guangxi, 537000, People's Republic of China; [4]Key Laboratory for Complementary and Alternative Medicine Experimental Animal Models of Guangxi, Nanning, Guangxi, 530299, People's Republic of China; [5]Guangxi Key Laboratory of Translational Medicine for Treating High-Incidence Infectious Diseases with Integrative Medicine, Nanning, Guangxi, 530299, People's Republic of China; [6]College of Pharmacy, Guangxi University of Chinese Medicine, Nanning, Guangxi, 530299, People's Republic of China

*These authors contributed equally to this work

Correspondence: Guanyi Wu, College of Basic Medicine, Guangxi University of Chinese Medicine, Nanning, Guangxi, 530299, People's Republic of China, Email wugy@gxtcmu.edu.cn

Purpose: Psoriasis is an immune-related disorder characterized by silver scales, epidermis thickness, and itching. She-Chuang-Si-Wu-Tang (SSWT), a traditional Chinese medicine decoction, has been used clinically for 400 years. Although it benefits psoriasis treatment, the mechanism of action is still unclear. This study explores SSWT's molecular mechanism in treating psoriasis through network pharmacology analysis and experiments.

Methods: We identified relevant SSWT and psoriasis targets using network pharmacology and conducted SSWT quality control with high-performance liquid chromatography (HPLC). A mouse model of psoriasis was established using imiquimod (IMQ), with the drug administered continuously for seven days, spanning an eight-day period. During the experiment, we observed spontaneous scratching behaviors and assessed the Psoriasis Area and Severity Index (PASI) scores. At the conclusion of the experiment, we examined skin tissue pathology under an optical microscope and measured epidermal thickness. Additionally, we used enzyme-linked immunosorbent assay (ELISA) and quantitative reverse transcription polymerase chain reaction (qRT-PCR) to measure interleukin (IL)-23, IL-17A, IL-17F, and interferon (IFN)-γ levels in the mice's serum and their mRNA expression in the skin. Western blot analysis was conducted to assess protein levels related to signaling pathways.

Results: Results indicate that SSWT may target IL-17 signaling pathways and T helper (Th) 17 cell differentiation, as predicted by network pharmacology. SSWT significantly improved the PASI and Baker scores, reduced epidermal thickness, and decreased spontaneous scratching in IMQ-induced mice. Additionally, SSWT treatment significantly lowered the concentrations of inflammatory factors in the serum and skin lesions, as well as mRNA expression levels, compared to the IMQ group. Furthermore, SSWT significantly inhibited the phosphorylation of both the signal transducer and activator of transcription 3 (STAT3) and mitogen-activated protein kinase (MAPK) pathways.

Conclusion: In summary, this study unveiled the potential anti-psoriatic mechanism of SSWT, offering new evidence for its clinical application.

Keywords: She-Chuang-Si-Wu-Tang, psoriasis, inflammation, itch, STAT3, MAPK

Received: 5 June 2024
Accepted: 28 August 2024
Published: 3 September 2024

Graphical Abstract

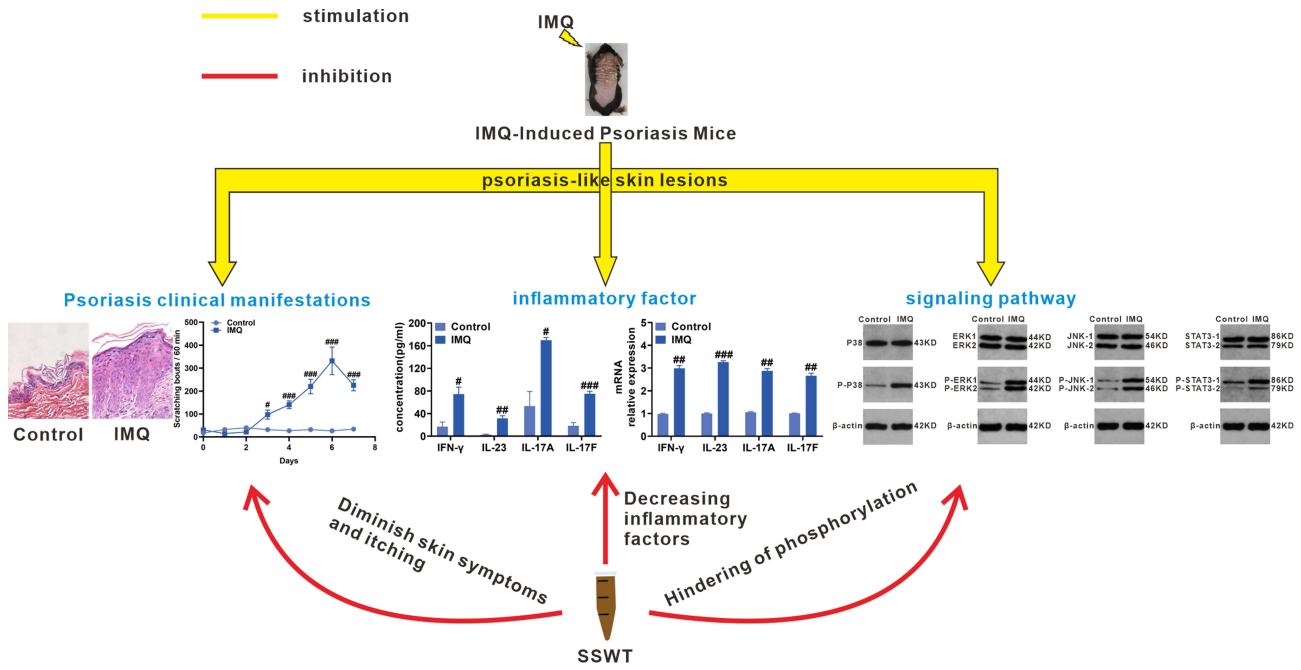

Introduction

Psoriasis is an immune-mediated inflammatory skin disorder affecting approximately 1% to 3% of the global population.[1] Characterized by silvery scales, thickened skin, and red patches, psoriasis can impact various body areas. Its pathogenesis involves immune cell activation and a surge in inflammatory cytokines, with the interleukin (IL)-23/IL-17 cytokine axis being central to this process.[2] IL-17, produced by T helper (Th) 17 cells under the influence of IL-23, acts as a pro-inflammatory mediator, promoting abnormal keratinocyte differentiation and proliferation.[3] Extensive research highlights the role of inflammation-related pathways, particularly the mitogen-activated protein kinase (MAPK) and signal transducer and activator of transcription 3 (STAT3) pathways, in psoriasis pathogenesis. These pathways regulate the release of inflammatory cytokines, cellular proliferation, differentiation, gene expression, and apoptosis.[4–6] Key components of the MAPK pathway, including p38, c-Jun N-terminal kinase (JNK), and extracellular signal-regulated kinase (ERK) 1/2, are involved in phosphorylation processes that enhance the expression of major inflammatory cytokines such as IL-17, IL-23, and Interferon (IFN)-γ.[7,8] Repeated phosphorylation of STAT3 can lead to psoriasis-like skin lesions in mice, while inhibiting STAT3 phosphorylation significantly improves these lesions.[9] STAT3 phosphorylation exacerbates psoriasis progression by disrupting γδT cells and enhancing IL-17 production in the skin.[10]

Psoriasis often recurs and requires long-term management. Treatment options include systemic medications (methotrexate, dexamethasone, tacrolimus), topical treatments (corticosteroids, vitamin D analogs), oral medications (apremilast, acitretin), and phototherapy (UVA, UVB).[11] Recent treatments using biologics, such as IL-17 inhibitors (secukinumab, ixekizumab) and IL-23 inhibitors (ustekinumab, guselkumab), have significantly improved Psoriasis Area and Severity Index (PASI) scores and patients' quality of life.[12] However, adverse reactions, resistance, long-term safety concerns, and high costs limit their widespread use and patients' adherence.[13] Traditional Chinese Medicine (TCM), with its multi-target effects, low side effects, and long-term safety, may offer a more effective and safer alternative for psoriasis treatment.

She-Chuang-Si-Wu-Tang (SSWT), as documented in "The Orthodox Manual of External Medicine", offers diverse benefits for conditions such as scrotal eczema, atopic dermatitis (AD), and pruritus vulvae, highlighting its biological and pharmacological properties.[14] The four herbs in SSWT are known for their anti-inflammatory properties, particularly *Cnidium monnieri*, which inhibits AD-like inflammation through coumarin compounds.[15–17] Additionally, oxymatrine

from *Sophora flavescens* and compounds from *Angelica sinensis* alleviate psoriasis-like symptoms by modulating specific inflammatory pathways.[18] Notably, *Angelica sinensis*, also a component of Dang-Gui-Liu-Huang Tang, reduces imiquimod (IMQ)-induced psoriasis-like inflammation in mice by suppressing IL-22 production, highlighting its importance in treating inflammatory skin conditions.[19] Currently, limited research exists on SSWT related to psoriasis, and its potential warrants further exploration.

Network pharmacology, grounded in systems biology and employing bioinformatics, uncovers the intricate network connections between drug targets and diseases. This aligns with the holistic approach of TCM, providing a novel method for uncovering mechanisms in Chinese herbal medicine that are multi-component, multi-target, and multi-pathway. This study employs network pharmacology to predict SSWT's potential mechanisms in treating psoriasis and validates its effects using IMQ-induced mice, laying a theoretical foundation for further research into SSWT's role in psoriasis treatment.

Material and Methods

Preparation of SSWT

SSWT is composed of Cnidium monnieri, *Sophora flavescens,* Clematis chinensis, and *Angelica sinensis* (Figure 1A). Table 1 shows the sources and composition of SSWT. SSWT was prepared according to the Chinese Pharmacopoeia (2015 Edition). The herbs were soaked for 30 minutes in 850 mL of water, then boiled at 100°C for 50 minutes. The mixture, once strained, was boiled again in 600 mL of water for 50 minutes. Decoctions from both boiling stages were collected, concentrated, and stored at 4°C (Figure 1B). The dose of SSWT for the experiment was determined using Jin's method.[20] Considering the average weights of an adult (70 kg) and a mouse (20 g), the dose ratio was calculated based on body surface area, resulting in a ratio of 0.0026.[21] For adults, the standard dosage of SSWT is 60 grams per day. Considering the weight of a mouse (20 g), the standard dosage for mice was calculated to be 7.8 g/kg, using the formula 60gx0.0026÷0.02kg. Specifically, the medium dose was set at 7.8 g/kg, the low dose at half that amount, and the high dose at twice the medium dose.

Network Pharmacology

We utilized the Traditional Chinese Medicine Systems Pharmacology (TCMSP) database (https://tcmsp-e.com/tcmsp.php) to identify the chemical components of four Chinese herbal medicines. We filtered these components to include only those with an oral bioavailability (OB) ≥ 30% and drug-likeness (DL) ≥ 0.18. Subsequently, we refined the targets and identified the active components and their corresponding targets of SSWT drugs using the STRING (https://string-db.org/) and UniProt (https://www.uniprot.org/) databases. To identify psoriasis-related targets, we searched for "psoriasis" in the GeneCard (https://www.genecards.org/) and DisGeNET (https://www.disgenet.org/) databases, and removed any duplicate targets. Venny 2.1.0 was used for Venn diagram analysis, comparing SSWT and psoriasis targets to identify potential targets for SSWT treatment of psoriasis. The common target genes were then imported into the STRING database to construct a protein-protein interaction (PPI) network, showing the connections and interactions among target genes, proteins, and molecules. We used Cytoscape 3.9.1 to construct a drug-compound-target network and performed topological analysis to obtain network-related information. In this network, nodes represented drug compositions, active components, and shared targets, while edges depicted the interactions within the network. KEGG and GO enrichment analyses were performed using the DAVID database (https://david.ncifcrf.gov/) and visualized with the Bioinformatics online mapping tool (http://www.bioinformatics.com.cn/). GO categorized key gene functions into cellular component (CC), molecular function (MF), and biological process (BP). KEGG enrichment analysis identified potential biological processes associated with the targets. The species parameter was set to "Homo sapiens", and a p-value of ≤0.05 was used as the significance threshold. After excluding tumor pathways, the results were ranked by p-value, showing the top 30 results from the GO and KEGG enrichment analyses.

Animal Model

C57BL/6J mice are sensitive to IMQ-induced psoriasis-like dermatitis and consistently exhibit pathological characteristics similar to human psoriasis, such as keratinocyte proliferation, inflammatory cell infiltration, and increased cytokine expression.[22] Therefore, C57BL/6J mice were selected for this study. Eighty C57BL/6J mice (17–22 g, 6–8 weeks old, male or female) were obtained from Hunan SJA Laboratory Animal Co., Ltd. (License No. SCXK (Hunan) 2019–0004).

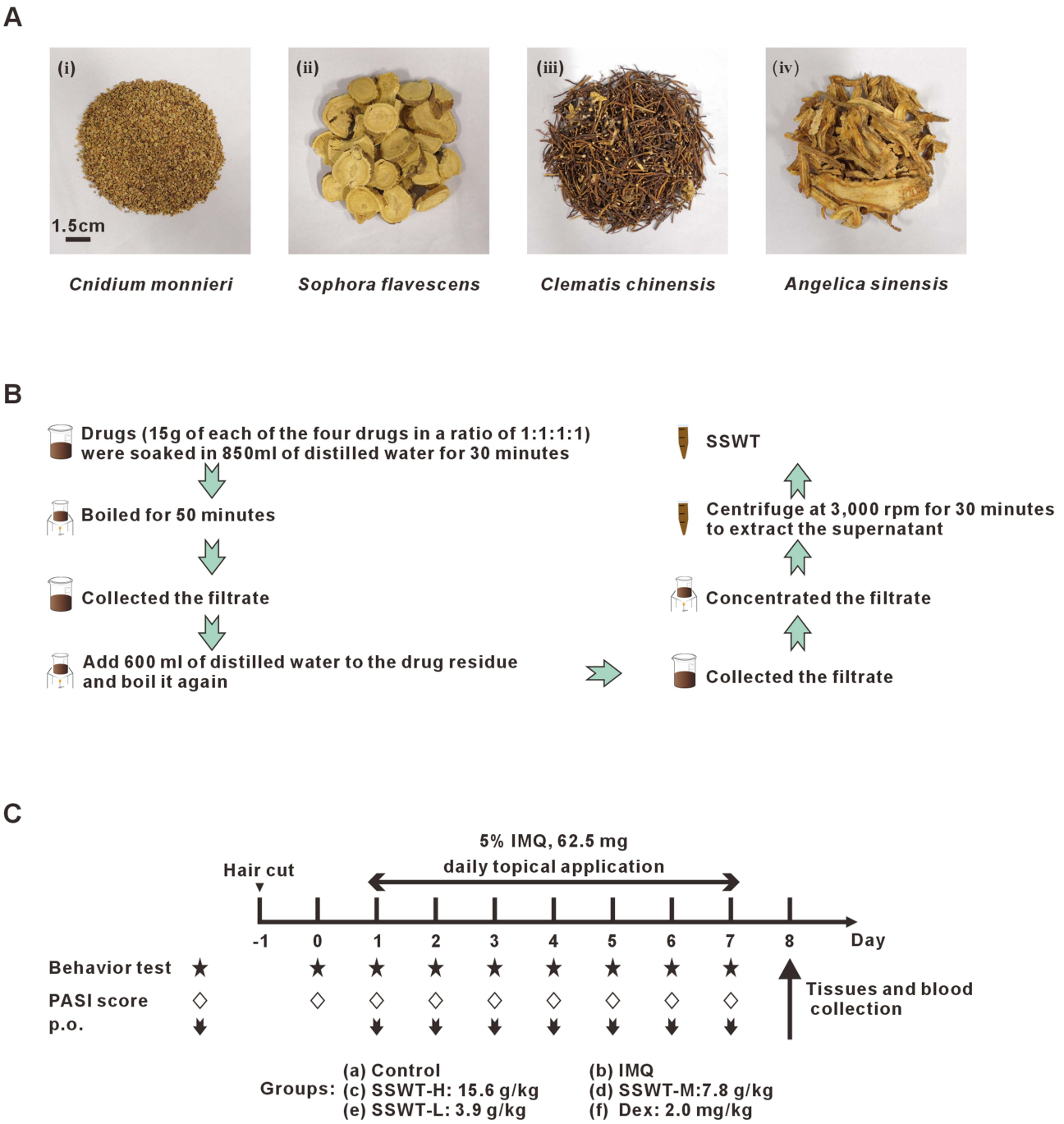

Figure 1 Preparing the SSWT and the experimental schedule. (**A**) SSWT is constituted by *Cnidium monnieri, Sophora flavescens, Clematis chinensis* and *Angelica sinensis*. (**B**) The SSWT preparation schedule. (**C**) The schematic diagram of the experimental procedure.

The mice were housed under specific pathogen-free (SPF) conditions at 23 ± 1°C with 40%-70% relative humidity and 12 hours of artificial light daily. All experiments were approved by the Institutional Animal Care and Use Committee of Guangxi University of Chinese Medicine (Ethics License No. DW20191220-153) and adhered to the "Guidelines for the Care and Use of Laboratory Animals." During the treatment period, each animal was housed individually in a standard cage. Non-toxic dye was applied to the hind limbs and tails of the mice to prevent licking and confusion.

Table 1 The Composition and Sources of SSWT

Botanical Name	Weight (g)	Place of Origin	Company
Cnidii fructus	15	Anhui, China	Xiushan Fuxingtong Decoction Pieces Co., Ltd
Sophorae flavescentis radix	15	Sichuan, China	Chengdu City Dujiangyan Chunsheng Chinese Medicine Drinks Co., Ltd.
Clematidis radix et rhizoma	15	Guangxi, China	Nanning Jingchang Chinese Medicine Tablet Co., Ltd.
Angelicae sinensis radix	15	Gansu, China	Gansu JoinNative Chinese Traditional MedicineIndustry Co., Ltd.

Animal Experiments

Mice were randomly divided into six groups: Control, IMQ, Dexamethasone (Dex), and three SSWT groups (low, medium, and high). Before the study, a 4.5 cm × 2.0 cm area on each mouse's back was shaved. For seven consecutive days, all groups except the control group received a daily application of 62.5 mg of 5% IMQ cream (Imiquimod, Minxinlidi Co. Ltd., Sichuan, China) on their backs. Four hours after IMQ application, the low-dose SSWT group (SSWT-L), medium-dose SSWT group (SSWT-M), and high-dose SSWT group (SSWT-H) were gavaged with 3.9 g/kg, 7.8 g/kg, and 15.6 g/kg of SSWT, respectively. The Dex group received 2 mg/kg Dex daily, while the IMQ and control groups were given distilled water. Spontaneous scratching behaviors were video-recorded for one hour after each day's treatment. Mice were placed in separate plastic chambers and acclimated for 15 minutes before observation. Scratching behavior was defined as lifting the hind limb toward the shaved neck area and then returning it to the floor. At the experiment's end, all mice were euthanized, and their dorsal skin, spleen, and whole blood were collected. The timeline of the animal experiment is shown in Figure 1C.

Psoriasis Area and Severity Index Assessment

The PASI was employed to evaluate the severity of skin inflammation. Erythema, scaling, and epidermal thickness were independently scored on a scale from 0 to 4, reflecting the degree of inflammation (0 = none, 1 = slight, 2 = moderate, 3 = marked, and 4 = very marked). Three researchers independently assessed each feature, and their scores were summed to produce a total score for each feature, ranging from 0 to 12. The cumulative scores for erythema, scaling, and thickening were then combined to represent the overall severity of inflammation, yielding a final score ranging from 0 to 36.

Histological Analysis

Dorsal skin samples were fixed in 4% paraformaldehyde and embedded in paraffin. Skin samples were then cut into 4 μm sections and stained with hematoxylin-eosin (HE) for light microscope histological observations (OLYMPUS, DP80). One image per tissue was taken at a 10×10 zoom and five images at a 40×10 zoom using CellSens Dimension software (n = 3 per group), both randomly. Epidermal thickness was randomly measured at four points on each image and averaged with Image J software. Pathological changes in skin tissue were observed under an optical microscope, with abnormalities evaluated using the Baker score, which ranges from 0 to 10.[23]

Wire Suspension Experiment

A wire suspension test assessed SSWT's effect on motor coordination. The wire suspension test included four groups: Control, SSWT-L, SSWT-M, and SSWT-H. Suspension tests were conducted 1 or 24 hours after SSWT or distilled water pretreatment on the mice. The test used a horizontal wire (100 cm × 2 mm) suspended 50 cm above padding. Mice were placed in the wire's middle and observed over three consecutive rounds at 120-second intervals. Mice staying on the wire for over 120 seconds or reaching its end scored 2, those remaining for 60–120 seconds scored 1, and those falling within 60 seconds scored 0 (n = 6 per group).

Open Field Experiment

An open-field test was conducted to assess SSWT's effect on locomotor activities and exploration. The open-field arena, measuring 62 cm × 62 cm × 30.5 cm, was constructed from a rectangular polymethylmethacrylate box, divided into sixteen equal-sized squares (15.5 cm × 15.5 cm). Mice were placed in the open field's center for spontaneous exploration

for five minutes after one or twenty-four hours of SSWT or distilled water pretreatment. A high-definition video recorded each mouse's total square crossings and front paw raisings.

Rotarod Experiment

An accelerated test was conducted to evaluate motor coordination. Mice underwent training three times daily for three consecutive days before the rotarod test. Mice were exposed to increasing rotarod speeds, from 4 to 5 RPM over five minutes, following 1 or 24 hours of SSWT or distilled water pretreatment. The time each mouse fell off the rotarod was recorded three times with five-minute intervals.

Enzyme-Linked Immunosorbent Assay (ELISA)

Serum was centrifuged at 3000 rpm and 4°C for 15 minutes, with the supernatant used for the ELISA test. IL-17A, IL-17F, IL-23, and IFN-γ levels were measured using ELISA kits (Bioswamp, China, and Multi Sciences, China) following the manufacturer's specifications. The OD value at 450 nm was measured using a microplate reader (BioTek, Epoch), after zeroing the blank control.

Quantitative Reverse Transcription Polymerase Chain Reaction (qRT-PCR) Gene Expression Analysis

Total RNA was extracted from skin samples using TRIzol reagent (Ambion, USA) following the manufacturer's instructions. Subsequently, RNA was reverse-transcribed to complementary deoxyribonucleic acids (cDNA) using reverse transcriptase (Vazyme, China). qRT-PCR was conducted using an EDC-810 real-time fluorescence PCR instrument (Eastwin, China) and the SYBR Green Master Mix kit (Vazyme, China). The β-actin gene served as a reference for normalizing experimental data. All data were analyzed using the $2^{-\Delta\Delta CT}$ method. The used primers are listed in Table 2.

Western Blot Assays

Skin samples were homogenized in RIPA lysis buffer (Beyotime, China). After centrifugation, the supernatant was collected, and the total protein concentration determined using the BCA protein concentration assay kit (Beyotime, Shanghai, China). Equal amounts of protein were separated by SDS-PAGE and transferred to a PVDF membrane (0.45

Table 2 Primer Sequences for Quantitative Reverse Transcription Polymerase Chain Reaction

Compounds	Primer	Sequence (5'-3')
osthole	Forward	CACGATGGAGGGGCCGGACTCATC
	Reverse	TAAAGACCTCTATGCCAACACAGT
matrine	Forward	CAGACTACCTCAACCGTTCC
	Reverse	AGCTTTCCCTCCGCATT
oxymatrine	Forward	CCAGGGTCAGGAAGACAGCA
	Reverse	GCAGCCAACTTTTAGGAGCA
caffeic acid	Forward	GCAGCTCTCTCGGAATCTCT
	Reverse	CGGGGCACATTATTTTTAGTC
ferulic acid	Forward	CGCTACACACTGCATCTTGG
	Reverse	TCCTTTTGCCAGTTCCTCCA

Abbreviations: SSWT, She-Chuang-Si-Wu-Tang; DCs, dendritic cells; ELISA, enzyme-linked immuno-sorbent assay; HE, hematoxylin-eosin; MAPK, mitogen-activated protein kinase; ERK, extracellular signal-regulating kinase; JNK, c-Jun N-terminal kinases; ANOVA, One-way analysis of variance; PASI, psoriasis area severity index; qRT-PCR, quantitative reverse transcription polymerase chain reaction; STAT3, signal transducer and activator of transcription 3; TCM, Traditional Chinese Medicine; TH, T helper; IMQ, imiquimod; IFN, interferon; IL, interleukin; Dex, dexamethasone; cDNA, complementary deoxyribonucleic acid; SEM, Standard Error of Mean; AD, Atopic dermatitis; HPLC, high-performance liquid chromatography; NF-kB, nuclear factor kappa B.

μm, Millipore, USA). The membrane was blocked with 5% skim milk powder for 2 hours, then incubated with primary antibodies overnight at 4°C. Enhanced chemiluminescence (ECL) was used to visualize target proteins after five TBST washes. Protein expression levels were measured with Image-Pro Plus (IPP), using β-actin as an internal standard.

High-Performance Liquid Chromatography Analysis of SSWT

Osthole, matrine, caffeic acid, oxymatrine, and ferulic acid, representing SSWT components,[24–26] are quality control standards, all purchased from Beijing Solarbio Science & Technology Co., with concentrations ≥98%. Following Zhang et al's method,[27] we quantified the five standards and SSWT-M (the standard clinical dose) using High-Performance Liquid Chromatography (HPLC) and compared the results. HPLC analysis used an Agilent 1260 Infinity II liquid chromatograph and a Hypersil Gold C18 column, with water for osthole, phosphate buffer for oxymatrine and matrine, and 0.1% aqueous phosphate solution for caffeic acid and ferulic acid as mobile phase A, and acetonitrile as mobile phase B. Elution was conducted using gradient or isocratic methods at a flow rate of 1.0 mL/min and an injection volume of 10 μL. Data were acquired and processed using OpenLab CDS Acquisition 2.5.0.842 and Agilent OpenLab Data Analysis 2.205.0.1344, respectively.

Statistical Analysis

All experimental data are presented as mean ± S.E.M. Statistical analysis was conducted with GraphPad Prism version 8.0.2. We used One-way analysis of variance (ANOVA) and the rank-sum test to analyze group differences. Differences between two groups were compared using Student's *t*-test. A p-value < 0.05 was considered statistically significant.

Results

Network Pharmacological Analysis

From the TCMSP database, we obtained 73 effective components and 215 corresponding targets. Combining psoriasis-related targets from the GeneCards and DisGeNET databases yielded a total of 5059 targets. A Venn diagram comparison of SSWT and psoriasis targets identified 148 common targets (Figure 2A). The effective components and common targets of SSWT treatment for psoriasis were imported into Cytoscape 3.8.0 to create a drug-disease intersection targets network, comprising 192 nodes and 511 edges (Figure 2B). In this network, pink hexagonal nodes represent drugs, pink diamond nodes signify SSWT's effective components, and blue hexagonal nodes denote action targets, illustrating SSWT's multi-component and multi-target characteristics for treating psoriasis. The 148 common targets were uploaded to the STRING database to create a PPI network (Figure 2C). After removing irrelevant targets, this network featured 147 nodes and 3689 edges. An average node degree of 50.19 and a local clustering coefficient of 0.71 suggest a strong inter-node association. Enrichment analyses of the 148 common targets were conducted using the DAVID database, resulting in 1005 targets with 778 in BP, 147 in MF, and 80 in CC, respectively. Figure 2D displays the top 30 significantly enriched genes. GO-BP analysis shows that target genes primarily participate in biological responses like responding to xenobiotic stimuli, positively regulating gene expression, and negatively regulating apoptosis. GO-MF reveals significant associations of target genes with enzyme binding, identical protein binding, and general protein binding. GO-CC demonstrates that target genes are primarily located in various cellular components, including the extracellular space, macromolecular complexes, and cytosol. Figure 2E presents the top 30 signaling pathways from KEGG analysis in a bubble chart. Considering their relevance to psoriasis, the IL-17 signaling pathway and Th17 cell differentiation were identified as the two most important signaling pathways. These findings suggest SSWT could treat psoriasis by influencing the IL-17 signaling pathway and Th17 cell differentiation.

High Performance Liquid Chromatograms of Five Representative Components in SSWT

HPLC was used to analyze and determine the standards and SSWT-M, with detection wavelengths for matrine and oxymatrine at 220 nm, caffeic acid at 316 nm, and ferulic acid and osthole at 322 nm, respectively (Figure 3A). Additionally, Figure 3B–F displays the chromatograms of the standards and SSWT-M. The results revealed that in SSWT-M, the retention times for osthole, matrine, oxymatrine, caffeic acid, and ferulic acid were 8.736, 11.826, 23.350,

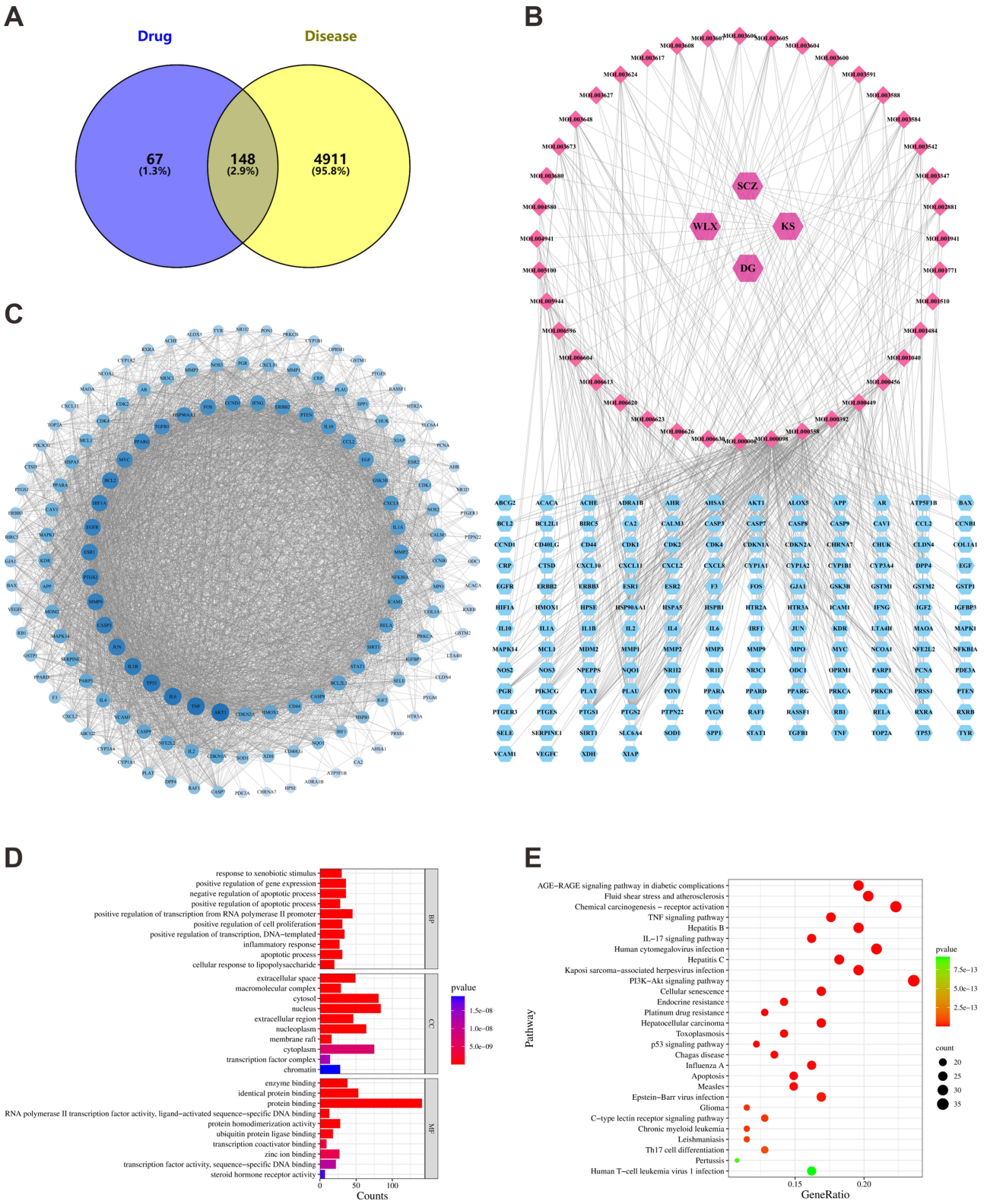

Figure 2 Employing network pharmacology to analyze the potential mechanisms of SSWT in treating psoriasis. (**A**) Venn diagram showing common targets of SSWT and psoriasis. (**B**) Psoriasis-target-SSWT network. (**C**) PPI network for common targets. (**D**) GO analysis results. (**E**) KEGG pathway enrichment results.

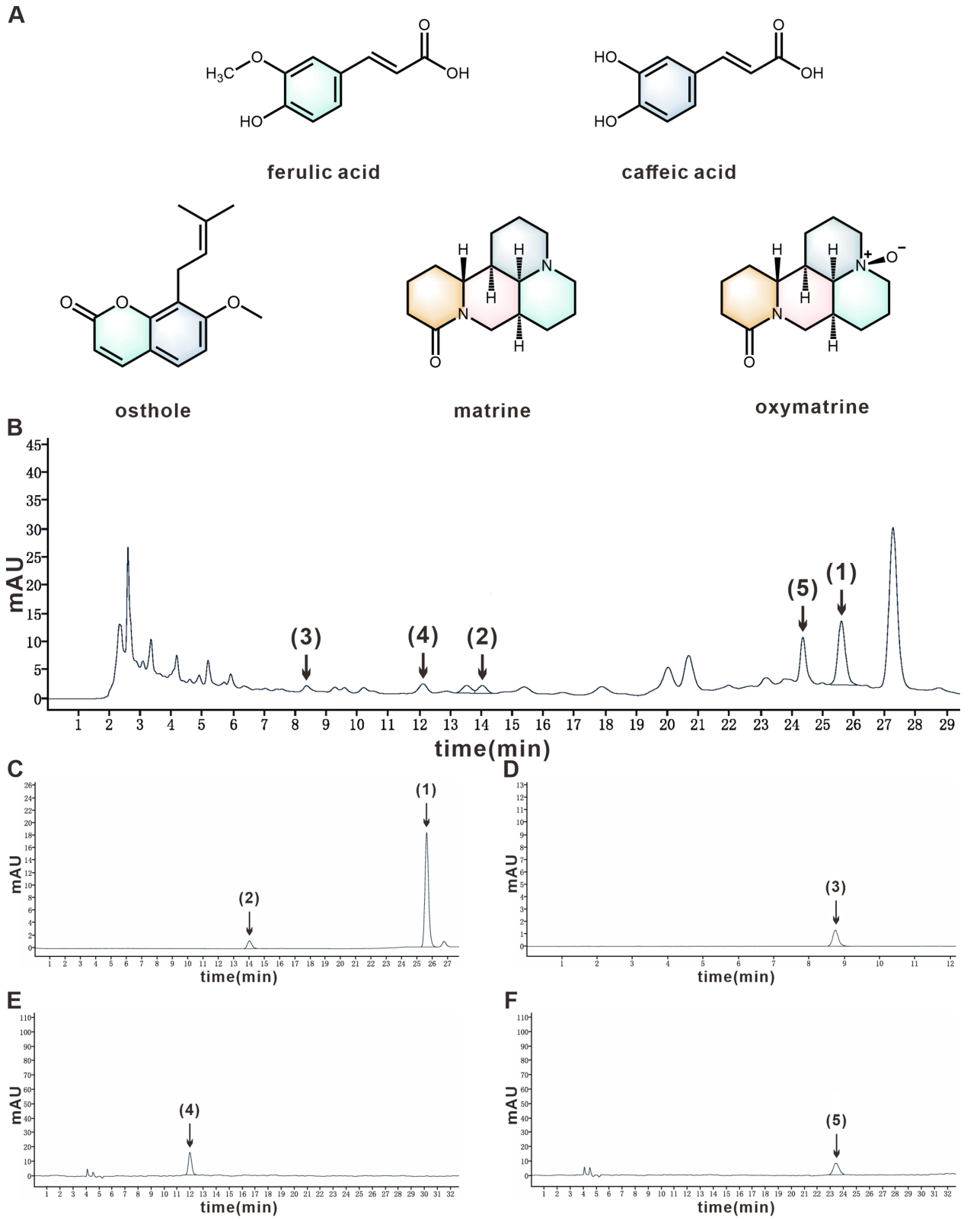

Figure 3 High-Performance Liquid Chromatography analysis of representative components in SSWT-M is performed. The chemical structures of ferulic acid, caffeic acid, osthole, matrine, and oxymatrine (**A**) and the high-performance liquid chromatogram of SSWT-M (**B**), where the representative components of the five Chinese herbal plants in the graph are ferulic acid (1), caffeic acid (2), osthole (3), matrine (4), and oxymatrine (5), are shown. The high-performance liquid chromatograms of the five control standards include ferulic acid, caffeic acid (**C**), osthole (**D**), matrine (**E**), and oxymatrine (**F**).

https://doi.org/10.2147/JIR.S472417 DovePress

14.009, and 25.586 minutes, respectively. The five chemical components' concentrations in SSWT were 0.470, 158.200, 9.444, 0.621, and 4.006 μg/mL, respectively.

The Effect of SSWT on the IMQ-Induced Morphological Changes of the Skin Lesions

We investigated the effects of SSWT on IMQ-induced skin lesions in a psoriasis-like mouse model by comparing morphological changes among the control, IMQ, and SSWT groups. The IMQ group exhibited erythema, scaling, and infiltration, while the control group showed no significant psoriasis-like lesions (Figure 4A and B). Significant reductions in erythema,

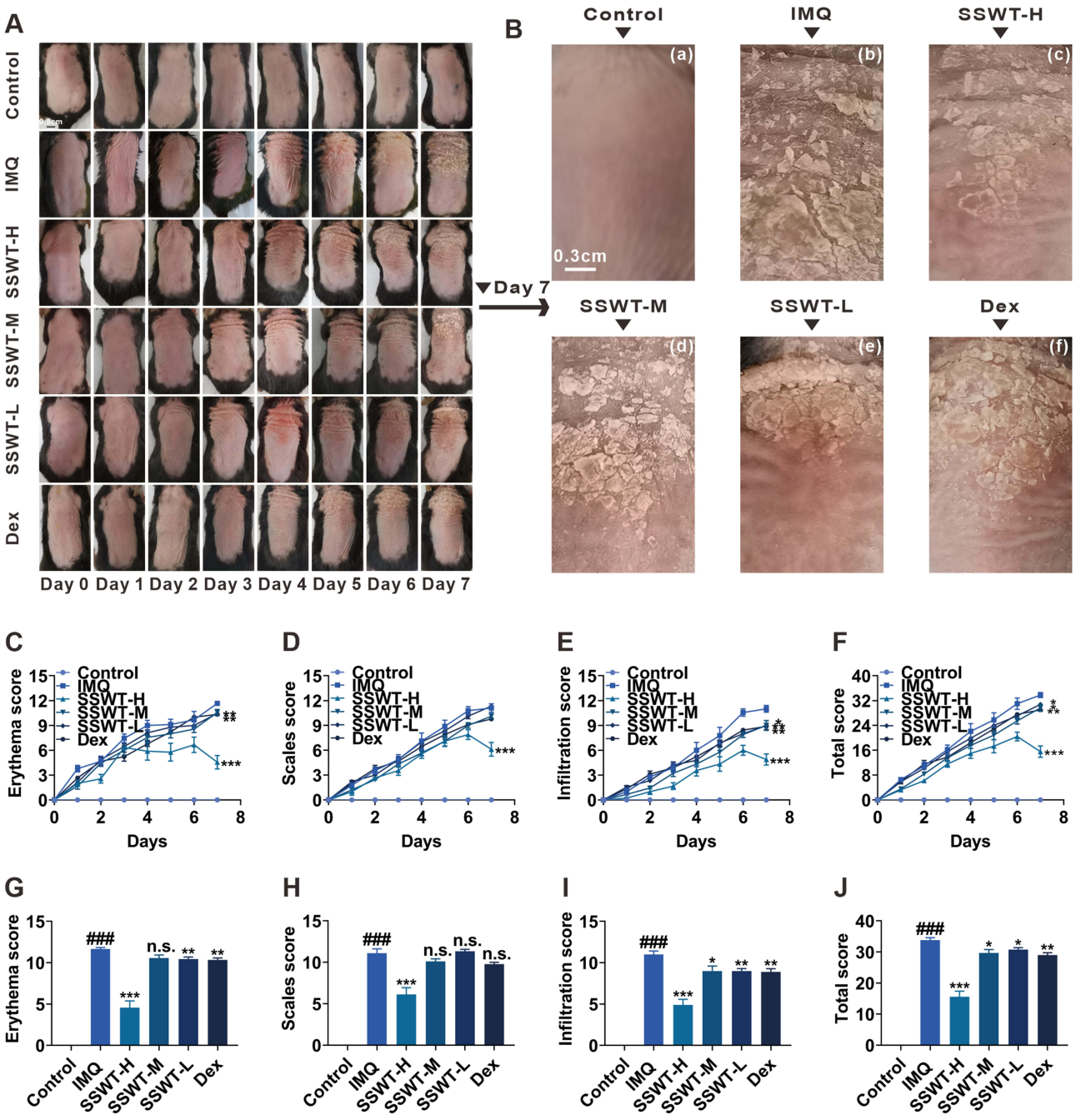

Figure 4 SSWT alleviated symptoms in IMQ-induced psoriasis-like mice. (**A**) The representative macroscopic views of the dorsal psoriatic skin lesions on Days 0–7 in each group. (**B**) The skin lesions from each group on Day 7. The erythema score (**C**), scaling score (**D**), infiltration score (**E**), and total score (**F**) in each group on Days 0–7. The erythema score (**G**), scaling score (**H**), infiltration score (**I**), and total score (**J**) in each group on Day 7. Data are represented as mean ± SEM (n = 8–9), $^{\#}p< 0.05$, $^{\#\#}p< 0.01$, $^{\#\#\#}p< 0.001$ vs the control; $^{*}p< 0.05$, $^{**}p< 0.01$, $^{***}p< 0.001$ vs the IMQ model.

Abbreviation: ns, no significant.

scaling, and skin infiltration were observed in the SSWT groups (Figure 4C–F). By Day 7, the PASI scores in the SSWT groups were significantly lower than those in the IMQ group (Figure 4G–J), with the most pronounced improvements seen in the high-dose SSWT group. These findings suggest that SSWT effectively alleviates IMQ-induced psoriatic inflammation.

The Effect of SSWT on Histopathology in IMQ-Induced Psoriasis-Like Mice

To further evaluate the effects of SSWT on histopathological features in IMQ-induced psoriatic mice, we analyzed HE stained dorsal skin samples from each group. The results revealed that the IMQ group had thicker epidermal acanthocyte layers, incomplete keratinization, and increased inflammatory cell infiltration compared to the control group, with the highest scores in the Baker scoring system. In the SSWT groups, Baker scores decreased in a dose-dependent manner compared to the IMQ group, with the high-dose SSWT group showing the greatest and statistically significant reduction (Figure 5A and B). Figure 5C shows that epidermal thickness in the SSWT groups decreased in a dose-dependent manner compared to the IMQ group, with statistically significant results. Therefore, SSWT resulted in histopathological improvements in mice with IMQ-induced psoriatic lesions.

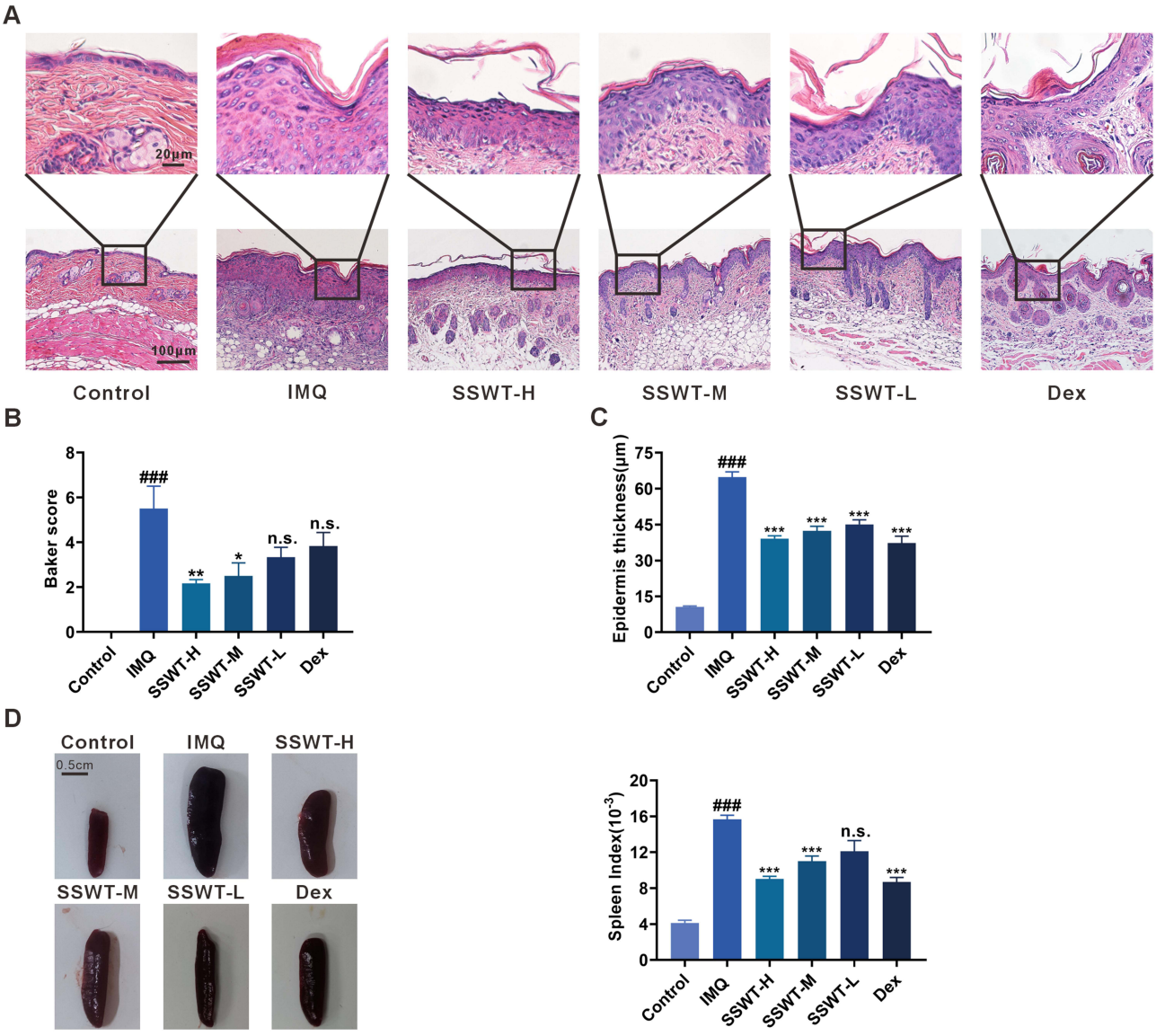

Figure 5 The effect of SSWT on the histopathological features and the spleen of IMQ-induced psoriasis-like mice. (**A**) The representative images of the back skin in each group, with HE staining, are shown. (**B**) Histopathology scores (Baker score). Data is represented as mean ± SEM (n = 3). (**C**) The epidermal thickness of the skin lesions in each group of mice. Data is represented as mean ± SEM (n = 15). (**D**) Images of the spleen and the spleen indices for each group. Data are represented as mean ± SEM (n = 8–9), $^{\#}p< 0.05$, $^{\#\#}p< 0.01$, $^{\#\#\#}p< 0.001$ vs the control; $^{*}p< 0.05$, $^{**}p< 0.01$, $^{***}p< 0.001$ vs the IMQ model.

Abbreviation: ns, no significant.

The Effect of SSWT on Spleen Enlargement in IMQ-Induced Psoriasis-Like Mice

We tested the spleen index to investigate the potential effect of SSWT on spleen enlargement. As shown in Figure 5D, the spleens in the IMQ group were significantly larger than those in the control group. In contrast, SSWT treatment reduced spleen size and weight in a dose-dependent manner when compared to the IMQ group. These findings suggest that SSWT mitigates IMQ-induced immune responses.

The Effect of SSWT on Spontaneous Scratching Behaviors in IMQ-Induced Psoriasis Mice

To assess the anti-pruritic effect of SSWT, we recorded spontaneous scratching behaviors in IMQ-induced psoriatic mice over eight days (Figure 6A). Results showed a significant increase in spontaneous scratching in the IMQ-treated mice from Day 3 compared to the control group. Additionally, scratching behaviors significantly decreased in the SSWT-H and

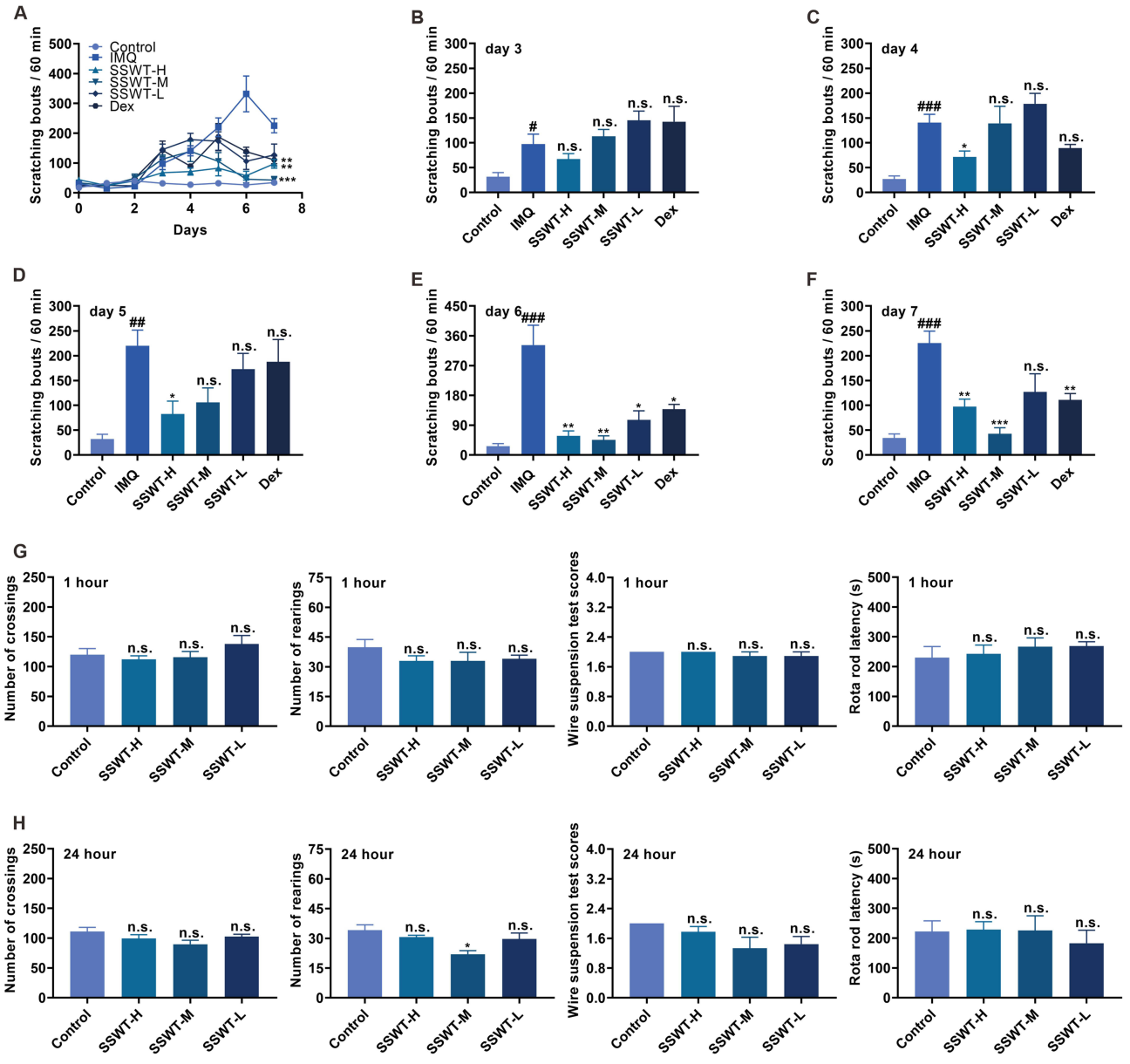

Figure 6 The effects of SSWT on mice's scratching behaviors, locomotion, exploration, and motor coordination. (**A**) The number of scratching for each group from Day 0 to Day 7, and the specific scratch counts on Day 3 (**B**), Day 4 (**C**), Day 5 (**D**), Day 6 (**E**), and Day 7 (**F**). Data are represented as mean ± SEM (n = 8–9), $^{\#}p< 0.05$, $^{\#\#}p< 0.01$, $^{\#\#\#}p< 0.001$ vs the control; $^{*}p< 0.05$, $^{**}p< 0.01$, $^{***}p< 0.001$ vs the IMQ model. Record the data from the Open Field Experiment, Wire Suspension Test, and Rotarod Experiment in mice that were treated with SSWT for 1 hour (**G**) and 24 hours (**H**). Data are represented as mean ± SEM (n = 6), $^{*}p< 0.05$, $^{**}p< 0.01$, $^{***}p< 0.001$, compared to the control.
Abbreviation: ns, no significant.

SSWT-M groups from Day 4 to Day 7 compared to the IMQ group (Figure 6B–F). Notably, the medium-dose SSWT treatment showed a more pronounced effect after Day 6. These findings suggest that SSWT effectively reduces spontaneous scratching in IMQ-induced psoriatic mice.

The Effect of SSWT on Locomotor Activities, Exploration, and Motor Coordination

We conducted the Wire Suspension Test, Open Field Test, and Rotarod Experiment to explore SSWT's potential impact on locomotion, exploration, and motor coordination in mice. Figure 6G, H shows that 1 and 24 hours after SSWT pretreatment, there were no significant differences in crossing, rearing, falling times from the Rotarod, or Wire Suspension Test scores between SSWT and control groups. These findings suggest that SSWT did not impact locomotion, exploration, or motor coordination in the psoriasis mouse model.

The Effect of SSWT on the Levels of Inflammatory Cytokines in IMQ-Induced Psoriasis Mice

To determine if SSWT can lower psoriasis-related inflammatory cytokine levels in IMQ-induced psoriatic mice, we assessed cytokine concentrations and mRNA levels in serum and skin. Figure 7A–H demonstrates that concentrations and mRNA expression levels of IFN-γ, IL-23, IL-17A, and IL-17F were significantly higher in IMQ-induced mice compared to the control group. However, SSWT significantly reduced IMQ-induced release and mRNA expression of IFN-γ, IL-23, IL-17A, and IL-17F in a dose-dependent manner. These findings suggest that SSWT suppresses inflammatory responses in mice with IMQ-induced psoriasis.

The Effect of SSWT on the Activation of the MAPK and STAT3 Signaling Pathways in IMQ-Induced Psoriatic Mice

The STAT3 and MAPK signaling cascades regulate the expression of inflammatory cytokines. We used Western blots to investigate the effect of SSWT on STAT3 and MAPK signaling protein levels in the skin of IMQ-induced psoriatic mice. As shown in Figure 8A–L, the protein expressions of p-STAT3, p-P38, p-ERK1/2, and p-JNK were significantly higher in the IMQ group than in the control group. SSWT treatment significantly reduced the levels of

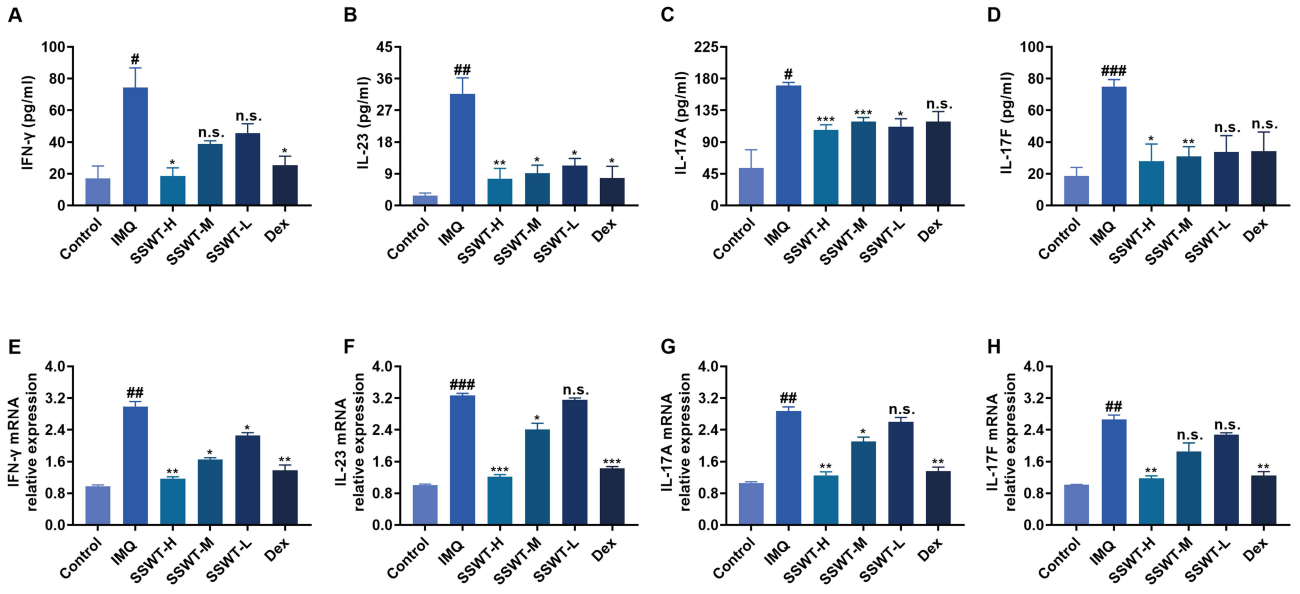

Figure 7 The effect of SSWT on the pro-inflammatory cytokine levels and the mRNA expressions of IMQ-induced psoriasis-like mice. The serum pro-inflammatory cytokines IFN-γ (**A**), IL-23 (**B**), IL-17A (**C**), and IL-17F (**D**) were measured using ELISA. Data are represented as mean ± SEM (n = 4–5). The mRNA levels of IFN-γ (**E**), IL-23 (**F**), IL-17A (**G**), and IL-17F (**H**) in the skin were measured by qRT-PCR. Data are represented as mean ± SEM (n = 3), $^{\#}p< 0.05$, $^{\#\#}p< 0.01$, $^{\#\#\#}p< 0.001$ vs the control; $^{*}p< 0.05$, $^{**}p< 0.01$, $^{***}p< 0.001$ vs the IMQ model.

Abbreviation: ns, no significant.

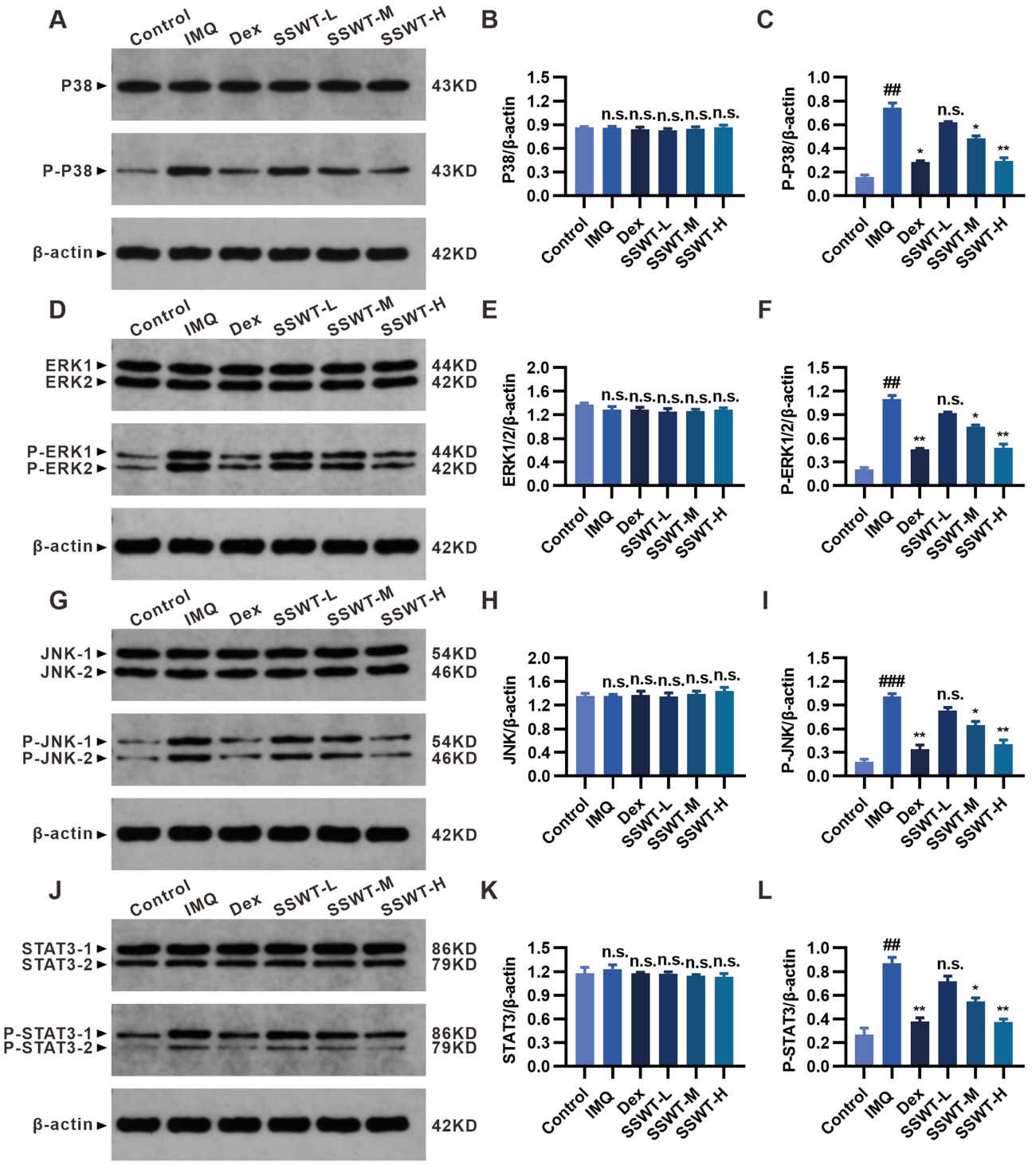

Figure 8 The effect of SSWT on the MAPK and STAT3 pathway components. The protein ex-pression levels of P38, p-P38 (**A**), ERK1/2, p-ERK1/2 (**D**), JNK, p-JNK (**G**), STAT3, and p-STAT3 (**J**) in the skin were measured by Western blot. Evaluation of P38(**B**), p-P38(**C**), ERK1/2(**E**), p-ERK1/2(**F**), JNK(**H**), p-JNK(**I**), STAT3(**K**), and p-STAT3(**L**) expression levels using ImageJ. Data are represented as mean ± SEM (n = 3), $^{\#}p< 0.05$, $^{\#\#}p< 0.01$, $^{\#\#\#}p< 0.001$ vs the control; $^{*}p< 0.05$, $^{**}p< 0.01$, $^{***}p< 0.001$ vs the IMQ model.
Abbreviation: ns, no significant.

these proteins in a dose-dependent manner compared to the IMQ group. These findings indicate that SSWT inhibits the activation of the STAT3 and MAPK signaling pathways, thereby regulating the expression of IMQ-induced cytokines and chemokines.

Discussion

Psoriasis is characterized as a chronic, inflammatory, papulosquamous skin disease with erythema and scales. The pathogenesis of psoriasis involves inflammatory cytokines and the disruption of the skin barrier. Orchestrated inflammatory cytokines damage the skin barrier, while lesioned skin further promotes inflammatory cytokine release, creating a vicious cycle. Thus, relieving skin inflammation is a strategic approach for treating psoriasis. The side effects and high costs of psoriasis medications pose challenges for patients. TCM offers an alternative treatment for psoriasis using complementary methods. Additionally, TCM has demonstrated greater efficacy and fewer side effects.

The term "psoriasis" originates from the Greek word "Psora", "signifying" "pruritus" when referred to in scholarly language. Past reports (from 1977 to 2017) on psoriasis patients reveal that about 60% to 90% exhibit clinical pruritus manifestations.[28] Amatya and Yosipovitch have demonstrated that itching is among the most painful and troublesome psoriasis symptoms.[29,30] Commonly used antipruritic therapies for psoriasis are recognized to be not fully effective, with potential weak effects or short-lived durations. Additionally, chronic use of these medications may lead to high risk adverse reactions, including infection and hepatotoxicity. Herbal formulations offer relevant alternative treatment options, with advantages like fewer side effects and lower costs. This study demonstrated a reduction in IMQ-induced spontaneous scratching behaviors with SSWT use. Thus, SSWT could offer a new approach for treating psoriasis induced itch symptoms.

IMQ acts as an inflammation and immune activator, stimulating monocytes, macrophages, and dendritic cells (DCs) to induce psoriatic skin inflammation in mouse models. A preliminary study found that,[31] after seven days of IMQ application, mice exhibited erythema, white scales, and thickened skin. This study showed that SSWT significantly reduced IMQ-induced PASI scores. Additionally, SSWT can treat splenomegaly and inhibit systemic immune responses. Histopathological analysis showed that SSWT treatment significantly reduced parakeratosis, thickened epidermal acanthocyte layers, and inflammatory cell infiltration in psoriatic mice, thereby lowering Baker scores. These findings suggest that SSWT reduces keratinocyte proliferation and inflammatory cell infiltration, potentially exerting an anti-inflammatory effect in IMQ-induced psoriasis in mice.

The analysis of the drug-disease intersection targets network reveals that SSWT components are complex, targets are diverse, and action pathways are extensive. The therapeutic effects of SSWT result from the combined actions of multiple active components. Certain constituents of SSWT, such as *Cnidium monnieri, Sophora flavescens*, and *Angelica sinensis*, possess anti-inflammatory properties. Osthole, *Cnidium monnieri*'s main active component, inhibits nuclear factor kappa B (NF-kB) and MAPK activation, displaying an anti-inflammatory effect both in vivo and in vitro.[32] Matrine and oxymatrine, the primary alkaloids in *Sophora flavescens*, help improve IMQ-induced psoriatic dermatitis.[33,34] *Angelica sinensis* reduces pro-inflammatory factors by blocking the NF-kB and MAPK pathways.[35] While SSWT's effect on psoriasis goes beyond a simple mix of TCM ingredients, their anti-inflammatory properties may enhance its anti-psoriatic efficacy.

Dex, an effective treatment for psoriasis,[36] was used as the standard treatment in this study to evaluate its effects on reducing inflammation and relieving itching. Our results showed that Dex significantly reduced the mRNA expression levels of IL-23, IL-17A, IL-17F, and IFN-γ, effectively alleviating the inflammatory response and itching symptoms in psoriasis mouse model, consistent with previous findings.[1] Dex is crucial in psoriasis treatment by inhibiting T cell activation and proliferation and reducing the release of inflammatory factors. Our study also found that SSWT was superior to Dex in reducing scratching behavior and skin lesions, with fewer side effects. These advantages suggest that SSWT may be a better treatment option, considering long-term efficacy and safety.

KEGG enrichment analysis shows that SSWT primarily targets psoriasis through Th17 cell differentiation and the IL-17 signaling pathway, which are interrelated. The Th17/IL-17 pathway plays a role in both the development and progression of psoriasis. IL-23, essential for starting the immune-inflammatory process, is produced by DCs and targets the IL-23 Receptor (IL-23R) on Th17 Cells.[37] IL-23 regulates the development, proliferation, and IL-17 secretion in Th17 cells.[38,39] IL-23 activates the Th17 pathway mainly through STAT3, which controls the transcription of key inflammatory mediators.[40] STAT3 regulates Th17 cell differentiation and cytokine secretion, including IL-23, IL-17A, and IL-17F, which use the STAT3 pathway to transmit signals, thus influencing psoriasis development and Th17 cell activation.[41] The STAT3 pathway can cause keratinocytes to over-proliferate and produce more IL-17, creating a feedback loop that further activates the TH17 and STAT3 pathways.[42] Additionally, STAT3 activates genes that regulate HaCaT cell proliferation and apoptosis, affecting feedback loops.[43] The

initiation of the MAPK pathway incites inflammatory reactions, playing a pivotal role in the development of psoriasis.[44] Within psoriatic lesions, there is a marked increase in the activation levels of p38, ERK1/2, and JNK. The movement of Th17 cells, which are crucial in driving inflammation, is particularly reliant on p38. Therefore, targeting and inhibiting the MAPK p38 pathway emerges as a strategic approach to control Th17-mediated inflammatory conditions.[45] Furthermore, suppressing the MAPK ERK pathway reduces keratinocyte proliferation.[46] JNK is essential for keratinocyte differentiation and proliferation, highlighting its role in psoriasis pathology.[47] In psoriasis models, overactive DCs stimulate Th cells to secrete IFN-γ, IL-17A, IL-17F, leading to excessive epidermal proliferation and chemokine and antimicrobial peptide secretion by keratinocytes, thus promoting psoriasis.[48] Gottlieb demonstrated significant improvement in inflammation and itch in patients using an IL-17 receptor antagonist.[49] This study found SSWT significantly reduced the release and mRNA expression of IL-17A, IL-17F, IL-23, and IFN-γ compared to the IMQ group. Western blotting detected protein levels of STAT3 and MAPK pathway components in mouse dorsal skin. Our findings reveal that IMQ application increased the phosphorylation of STAT3, P38, JNK, and ERK1/2, thus activating the STAT3 and MAPK pathways. Concurrently, SSWT treatment countered IMQ's effects by reducing the phosphorylation of STAT3, P38, JNK, and ERK1/2, thereby inhibiting the STAT3 and MAPK pathways. Our results suggest that SSWT improves IMQ-induced psoriatic lesions, reduces scratching, and alleviates inflammation. The potential mechanism likely involves regulating Th17 cell differentiation and the IL-17 signaling pathway through the STAT3 and MAPK pathways, consistent with KEGG analysis predictions. In the future, SSWT could become an effective treatment for psoriasis or a key component in combination therapies due to its unique multi-target and multi-pathway actions that enhance efficacy and minimize side effects. Additionally, SSWT can serve as a valuable source for drug development. Single compounds extracted from TCM, when processed through modern drug development procedures, hold potential as innovative treatments for psoriasis. However, this study has limitations. The main active components of SSWT have not been identified, and the anti-psoriatic effects of other components remain unknown. Furthermore, the specific mechanisms of action, particularly SSWT's interactions with the STAT3 and MAPK pathways, are unclear and require further investigation.

Conclusion

In conclusion, this study confirmed the efficacy of SSWT in treating psoriasis and elucidated its underlying mechanisms. Network pharmacology demonstrated that SSWT improves psoriasis through the synergistic interaction of various components, targets, and pathways. In vivo trials showed that SSWT reduces epidermal thickness, alleviates itchiness, lowers PASI and Baker scores, and suppresses cytokine release and mRNA expression. SSWT's anti-inflammatory and antipruritic effects are mediated by its regulation of the STAT3/ MAPK pathways, impacting IL-17 signaling and Th17 cell differentiation. Thus, SSWT presents a promising alternative for psoriasis treatment. However, this study has several limitations. While in vivo trials provided valuable insights, clinical trials are needed to confirm SSWT's safety and efficacy in humans. Future clinical studies should focus on evaluating the long-term effects and potential side effects of SSWT. Additionally, although the anti-psoriatic effects of SSWT were identified, the specific active components were not. Future research should aim to isolate and identify these active components to enable more targeted therapeutic approaches. Moreover, the study primarily focused on the STAT3 / MAPK pathways, but other relevant pathways might also play crucial roles in SSWT's therapeutic effects, necessitating further exploration in future research.

Institutional Review Board Statement

All experiments were approved by the Institutional Animal Care and Use Committee of the Guangxi University of Chinese Medicine (Ethics license DW20191220-153).

Data Sharing Statement

All available data information is included in the article.

Author Contributions

All authors made a significant contribution to the work reported, whether that is in the conception, study design, execution, acquisition of data, analysis and interpretation, or in all these areas; took part in drafting, revising or critically

reviewing the article; gave final approval of the version to be published; have agreed on the journal to which the article has been submitted; and agree to be accountable for all aspects of the work.

Funding

This study was supported by the following: a Grant from the Natural Science Founda-tion of Guangxi Zhuang Autonomous Region (2020GXNSFAA297244); the Natural Science Foundation of China (NSFC) to Guanyi Wu (82060768); an Innovation Project of Guangxi Graduate Education (YCSW2023392); the Guipai Traditional Chinese Medicine Top-Notch Talent Funding Project from Guangxi University of Chinese Medicine; the Second and Third Batch of the "Qihuang Project" High-Level Talent Team Cultivation Project of Guangxi University of Traditional Chinese Medicine (2021001, 202402); and a Student Innovation and Entrepreneurship Project of Guangxi University of Traditional Chinese Medicine (S202210600097).

Disclosure

The authors declare no competing financial interests or personal relationships that could influence the work reported in this paper.

References

1. Wang W, Wang H, Zhao Z, Huang X, Xiong H, Mei Z. Thymol activates TRPM8-mediated Ca2+ influx for its antipruritic effects and alleviates inflammatory response in Imiquimod-induced mice. *Toxicol Appl Pharmacol*. 2020;407:115247. doi:10.1016/j.taap.2020.115247
2. Lowes MA, Suárez-Fariñas M, Krueger JG. Immunology of Psoriasis. *Annu Rev Immunol*. 2014;32(1):227–255. doi:10.1146/annurev-immunol-032713-120225
3. OuYang Q, Pan Y, Luo H, Xuan C, Liu J, Liu J. MAD ointment ameliorates Imiquimod-induced psoriasiform dermatitis by inhibiting the IL-23/IL-17 axis in mice. *Int Immunopharmacol*. 2016;39:369–376. doi:10.1016/j.intimp.2016.08.013
4. Kyriakis JM, Avruch J. Mammalian MAPK signal transduction pathways activated by stress and inflammation: a 10-year update. *Physiol Rev*. 2012;92(2):689–737. doi:10.1152/physrev.00028.2011
5. Sun Y, Zhang J, Zhai T, et al. CCN1 promotes IL-1β production in keratinocytes by activating p38 MAPK signaling in psoriasis. *Sci Rep*. 2017;7(1):43310. doi:10.1038/srep43310
6. Wang A, Wei J, Lu C, et al. Genistein suppresses psoriasis-related inflammation through a STAT3–NF-κB-dependent mechanism in keratinocytes. *Int Immunopharmacol*. 2019;69:270–278. doi:10.1016/j.intimp.2019.01.054
7. Lin ZM, Ma M, Li H, et al. Topical administration of reversible SAHH inhibitor ameliorates imiquimod-induced psoriasis-like skin lesions in mice via suppression of TNF-α/IFN-γ-induced inflammatory response in keratinocytes and T cell-derived IL-17. *Pharmacol Res*. 2018;129:443–452. doi:10.1016/j.phrs.2017.11.012
8. Chuang SY, Chen CY, Yang SC, Alalaiwe A, Lin CH, Fang JY. 2,4-dimethoxy-6-methylbenzene-1,3-diol, a benzenoid from antrodia cinnamomea, mitigates psoriasiform inflammation by suppressing MAPK/NF-κB phosphorylation and GDAP1L1/Drp1 translocation. *Front Immunol*. 2021;12:664425. doi:10.3389/fimmu.2021.664425
9. Sano S, Chan KS, Carbajal S, et al. Stat3 links activated keratinocytes and immunocytes required for development of psoriasis in a novel transgenic mouse model. *Nat Med*. 2005;11(1):43–49. doi:10.1038/nm1162
10. Hartwig T, Pantelyushin S, Croxford AL, Kulig P, Becher B. Dermal IL-17-producing γδ T cells establish long-lived memory in the skin. *Eur J Immunol*. 2015;45(11):3022–3033. doi:10.1002/eji.201545883
11. Greb JE, Goldminz AM, Elder JT, et al. Psoriasis. *Nat Rev Dis Primers*. 2016;2(1):1–17. doi:10.1038/nrdp.2016.82
12. Campa M, Mansouri B, Warren R, Menter A. A review of biologic therapies targeting IL-23 and IL-17 for use in moderate-to-severe plaque psoriasis. *Dermatol Ther*. 2016;6(1):1–12. doi:10.1007/s13555-015-0092-3
13. Martins AM, Ascenso A, Ribeiro HM, Marto J. Current and future therapies for psoriasis with a focus on serotonergic drugs. *Mol Neurobiol*. 2020;57(5):2391–2419. doi:10.1007/s12035-020-01889-3
14. Chen X, Zhu C, Zhang Y, et al. Antipruritic effect of ethyl acetate extract from *fructus cnidii* in mice with 2,4-dinitrofluorobenzene-induced atopic dermatitis. *Evid Based Complement Alternat Med*. 2020;2020:1–14. doi:10.1155/2020/6981386
15. Lee TH, Chen YC, Hwang TL, et al. New coumarins and anti-inflammatory constituents from the fruits of cnidium monnieri. *IJMS*. 2014;15(6):9566–9578. doi:10.3390/ijms15069566
16. Tsai YF, Yu HP, Chung PJ, et al. Osthol attenuates neutrophilic oxidative stress and hemorrhagic shock-induced lung injury via inhibition of phosphodiesterase 4. *Free Radic Biol Med*. 2015;89:387–400. doi:10.1016/j.freeradbiomed.2015.08.008
17. Wang Z, Shen Y. The natural product osthole attenuates yeast growth by extensively suppressing the gene expressions of mitochondrial respiration chain. *Curr Microbiol*. 2017;74(3):389–395. doi:10.1007/s00284-016-1191-9
18. Xiang X, Tu C, Li Q, et al. Oxymatrine ameliorates imiquimod-induced psoriasis pruritus and inflammation through inhibiting heat shock protein 90 and heat shock protein 60 expression in keratinocytes. *Toxicol Appl Pharmacol*. 2020;405:115209. doi:10.1016/j.taap.2020.115209
19. Nguyen LTH, Ahn SH, Nguyen UT, Yang IJ. Dang-Gui-Liu-Huang Tang a traditional herbal formula, ameliorates imiquimod-induced psoriasis-like skin inflammation in mice by inhibiting IL-22 production. *Phytomedicine*. 2018;47:48–57. doi:10.1016/j.phymed.2018.04.051
20. Jin X, Xu H, Huang C, et al. A traditional Chinese medicine formula danshen baibixiao ameliorates imiquimod-induced psoriasis-like inflammation in mice. *Front Pharmacol*. 2021;12:749626. doi:10.3389/fphar.2021.749626

21. Li F, Yan H, Jiang L, Zhao J, Lei X, Ming J. Cherry polyphenol extract ameliorated dextran sodium sulfate-induced ulcerative colitis in mice by suppressing Wnt/β-catenin signaling pathway. *Foods*. 2022;11(1):49. doi:10.3390/foods11010049
22. van der Fits L, Mourits S, Voerman JSA, et al. Imiquimod-induced psoriasis-like skin inflammation in mice is mediated via the IL-23/IL-17 axis. *J Immunol*. 2009;182(9):5836–5845. doi:10.4049/jimmunol.0802999
23. Almudaris SA, Gatea FK. Effects of topical ivermectin on imiquimod-induced psoriasis in mouse model – novel findings. *PHAR*. 2024;71:1–14. doi:10.3897/pharmacia.71.e114753
24. Li X, Wu X, Huang L. Correlation between antioxidant activities and phenolic contents of radix angelicae sinensis (Danggui). *Molecules*. 2009;14 (12):5349–5361. doi:10.3390/molecules14125349
25. Yuan F, Chen J, Wj W, et al. Effects of matrine and oxymatrine on catalytic activity of cytochrome P450s in rats: MATRINE AND OXYMATRINE AND RAT CYPS. *Basic Clin. Physiol. Pharmacol.* 2010;107(5):906–913. doi:10.1111/j.1742-7843.2010.00596.x
26. Zhang ZR, Leung W, Li G, et al. Osthole enhances osteogenesis in osteoblasts by elevating transcription factor osterix via cAMP/CREB signaling in vitro and in vivo. *Nutrients*. 2017;9(6):588. doi:10.3390/nu9060588
27. Zhang X, Li X, Chen Y, et al. Xiao-Yin-Fang therapy alleviates psoriasis-like skin inflammation through suppressing γδT17 cell polarization. *Front Pharmacol*. 2021;12:629513. doi:10.3389/fphar.2021.629513
28. Elewski B, Alexis AF, Lebwohl M, et al. Itch: an under-recognized problem in psoriasis. *J Eur Acad Dermatol Venereol*. 2019;33(8):1465–1476. doi:10.1111/jdv.15450
29. Yosipovitch G, Goon A, Wee J, Chan YH, Goh CL. The prevalence and clinical characteristics of pruritus among patients with extensive psoriasis. *Br J Dermatol*. 2000;143(5):969–973. doi:10.1046/j.1365-2133.2000.03829.x
30. Amatya B, Wennersten G, Nordlind K. Patients' perspective of pruritus in chronic plaque psoriasis: a questionnaire-based study. *J Eur Acad Dermatol Venerol*. 2008;22(7):822–826. doi:10.1111/j.1468-3083.2008.02591.x
31. Zhou HF, Wang FX, Sun F, et al. Aloperine ameliorates IMQ-induced psoriasis by attenuating Th17 differentiation and facilitating their conversion to treg. *Front Pharmacol*. 2022;13:778755. doi:10.3389/fphar.2022.778755
32. Fan H, Gao Z, Ji K, et al. The in vitro and in vivo anti-inflammatory effect of osthole, the major natural coumarin from Cnidium monnieri (L.) Cuss, via the blocking of the activation of the NF-κB and MAPK/p38 pathways. *Phytomedicine*. 2019;58:152864. doi:10.1016/j.phymed.2019.152864
33. Jiang WW, Wang YM, Wang XY, Zhang Q, Zhu SM, Zhang CL. Role and mechanism of matrine alone and combined with Acitretin for HaCaT cells and psoriasis-like murine models. *Chinese Med J*. 2019;132(17):2079–2088. doi:10.1097/CM9.0000000000000412
34. Shi HJ, Zhou H, Ma AL, et al. Oxymatrine therapy inhibited epidermal cell proliferation and apoptosis in severe plaque psoriasis. *Br J Dermatol*. 2019;181(5):1028–1037. doi:10.1111/bjd.17852
35. Lee J, Choi YY, Kim MH, et al. Topical application of *angelica sinensis* improves pruritus and skin inflammation in mice with atopic dermatitis-like symptoms. *Journal of Medicinal Food*. 2016;19(1):98–105. doi:10.1089/jmf.2015.3489
36. Hogue L, Cardwell LA, Roach C, et al. Psoriasis and atopic dermatitis "resistant" to topical treatment responds rapidly to topical desoximetasone spray. *J Cutan Med Surg*. 2019;23(2):157–163. doi:10.1177/1203475418818082
37. Di Cesare A, Di Meglio P, Nestle FO. The IL-23/Th17 Axis in the Immunopathogenesis of Psoriasis. *J Invest Dermatol*. 2009;129(6):1339–1350. doi:10.1038/jid.2009.59
38. McGeachy MJ, Chen Y, Tato CM, et al. The interleukin 23 receptor is essential for the terminal differentiation of interleukin 17–producing effector T helper cells in vivo. *Nat Immunol*. 2009;10(3):314–324. doi:10.1038/ni.1698
39. Tonel G, Conrad C, Laggner U, et al. Cutting edge: a critical functional role for IL-23 in psoriasis. *J Immunol*. 2010;185(10):5688–5691. doi:10.4049/jimmunol.1001538
40. Sun W, Gao Y, Yu X, et al. 'Psoriasis 1' reduces psoriasis-like skin inflammation by inhibiting the VDR-mediated nuclear NF-κB and STAT signaling pathways. *Mol Med Rep*. 2018;18(3):2733–2743. doi:10.3892/mmr.2018.9262
41. Zhao J, Di T, Wang Y, et al. Multi-glycoside of tripterygium wilfordii hook. f. ameliorates imiquimod-induced skin lesions through a STAT3-dependent mechanism involving the inhibition of Th17-mediated inflammatory responses. *IntJ Mol Med*. 2016;38(3):747–757. doi:10.3892/ijmm.2016.2670
42. Xu F, Xu J, Xiong X, Deng Y. Salidroside inhibits MAPK, NF-κB, and STAT3 pathways in psoriasis-associated oxidative stress via SIRT1 activation. *Redox Rep*. 2019;24(1):70–74. doi:10.1080/13510002.2019.1658377
43. Yang Z, Chen Z, Wang C, Huang P, Luo M, Zhou R. STAT3/SH3PXD2A-AS1/miR-125b/STAT3 positive feedback loop affects psoriasis pathogenesis via regulating human keratinocyte proliferation. *Cytokine*. 2021;144:155535. doi:10.1016/j.cyto.2021.155535
44. Andrés RM, Hald A, Johansen C, Kragballe K, Iversen L. Studies of Jak/STAT3 expression and signalling in psoriasis identifies STAT3-Ser727 phosphorylation as a modulator of transcriptional activity. *Exp Dermatol*. 2013;22(5):323–328. doi:10.1111/exd.12128
45. Kadiri M, El Azreq MA, Berrazouane S, Boisvert M, Aoudjit F. Human Th17 Migration in Three-Dimensional Collagen Involves p38 MAPK: Th17 M IGRATION</sc> R EQUIRES p38. *J Cell Biochem*. 2017; 118(9): 2819–2827. doi:10.1002/jcb.25932
46. Wang Y, Han D, Huang Y et al. Oral administration of punicalagin attenuates imiquimod-induced psoriasis by reducing ROS generation and inflammation via MAPK / ERK and NF-κB signaling pathways.*Phytother Res*.2024;382:713–726.doi:10.1002/ptr.8071
47. Schumacher M, Schuster C, Rogon ZM, et al. Efficient keratinocyte differentiation strictly depends on JNK-induced soluble factors in fibroblasts. *J Invest Dermatol*. 2014;134(5):1332–1341. doi:10.1038/jid.2013.535
48. Wu R, Zeng J, Yuan J, et al. MicroRNA-210 overexpression promotes psoriasis-like inflammation by inducing Th1 and Th17 cell differentiation. *J Clin Investig*. 2018;128(6):2551–2568. doi:10.1172/JCI97426
49. Gottlieb A, Gratacos J, Dikranian A, et al. Treatment patterns, unmet need, and impact on patient-reported outcomes of psoriatic arthritis in the United States and Europe. *Rheumatol Int*. 2019;39(1):121–130. doi:10.1007/s00296-018-4195-x